Vietnam Journal of Earth Sciences, 45(4), 497-516, https://doi.org/10.15625/2615-9783/18923

Vietnam Journal of Earth Sciences
https://vjs.ac.vn/index.php/jse

Holocene sedimentary facies in the incised valley of Ma River Delta, Vietnam

Nguyen Minh Quang[1,2], Vu Van Ha[*1,2], Nguyen Thi Min[1], Ngo Thi Dao[1], Nguyen Thi Thu Cuc[3], Dang Minh Tuan[1], Dang Xuan Tung[1], Tran Thi Man[1], Nguyen Thi Thao[2,4]

[1]*Institute of Geological Sciences, VAST, Vietnam*
[2]*Graduate University of Science and Technology, VAST, Vietnam*
[3]*Hanoi University of Sciences, VNU*
[4]*Institute of Geography, VAST, Vietnam*

Received 27 October 2021; Received in revised form 27 July 2022; Accepted 15 September 2023

ABSTRACT

Holocene sediment facies in the incised valley of the Ma River Delta were clarified by using analysis of LKTH6 core (32 m depth) such as sedimentary structure analysis, grain-sized, micro-paleontological (foraminifera, spore and pollen, and diatom), clay minerals characteristics, and Radiocarbon dating (^{14}C). Ten sedimentary facies were identified, including (1) flood plain silty clay facies, (2) Salt marsh clayey silt facies, (3) Tidal flat sandy silty clay facies, (4) Tidal creek and tidal branch silty clayey sand facies, (5) Bay silty clay facies, (6) Prodelta silty clay facies, (7) Delta front silty sand facies, (8) Mouth bar sand facies, (9) Point bar silty sand faces, and (10) Alluvial plain silty clay facies.

The sea level change after the last glacial was recorded by sediment facies and radiocarbon dating (^{14}C). It showed that before 9380 yr. BP, the transgression concurrent with the base-level rising resulted in the incised valley filled up by fluvial sediment. The transgression drowned incised valley was recorded by the initial marine flooding surface which was identified by salt marsh sedimentary facies in the valley at 9380 yr. BP, and the drowning process of the incised valley completely around 8000 yr. BP. After 8000 yr. BP, the sedimentary accumulation exceeded the sea level rise rate resulting in the delta being formed.

Keywords: Holocene sedimentary facies, insiced valley, sea level change, Ma River Delta.

1. Introduction[1]

The Ma River Delta is the third largest delta in Vietnam (after the Mekong and Red River Deltas). The Ma River system originates from Dien Bien province, flows through the territory of Laos, and then back into Vietnam in the region of Thanh Hoa province. It flows into three estuaries, Lach Truong, Len, and Hoi, where Hoi's mouth is the largest (Fig. 1). During the Late Pleistocene, the global sea level dropped from 100 to 120 m during the Wurm glaciation (Ha, 2015; Lam, 2004, 2003). Weathering and erosion dominated the entire coastal Thanh Hoa area in the Late Pleistocene (before the Flandrian transgression sea level), with profound cleavage in the estuaries and forming the Late Quaternary incised valley. They stretch from Lach Truong estuary in the Hau Loc district and upstream in the Southeast-Northwest direction with 41 m depth (Fig. 2, Table 1) (Quang, 2022).

*Corresponding author, Email: vuha@igsvn.vast.vn

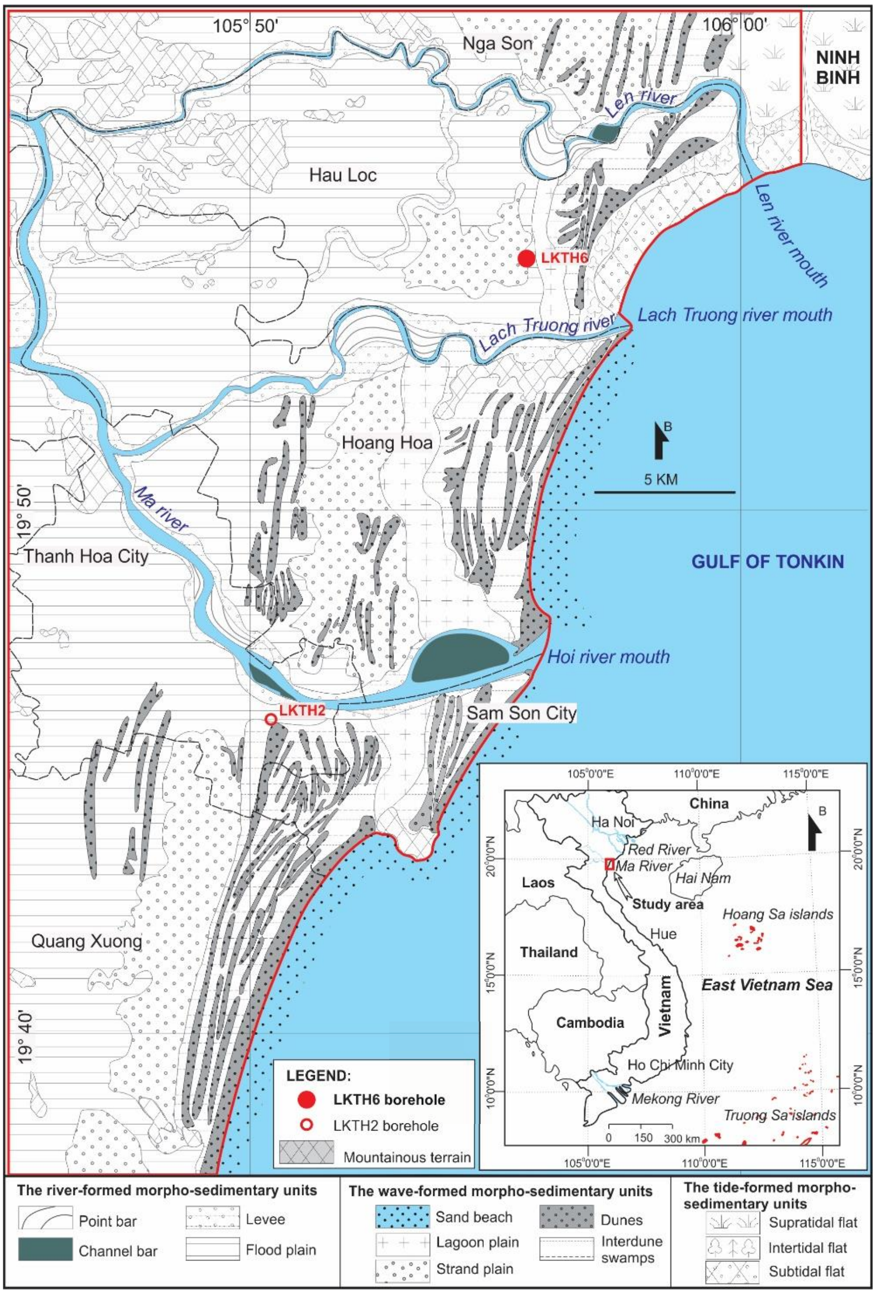

Figure 1. Geomorphologycal map of coastal Thanh Hoa area (Quang et al., 2021; Quang, 2022) and the LKTH6 core

The previous studies carried out in the area mainly geological mapping at 1:200000 scale (Quan and Chu, 1980) and Thanh Hoa urban geological investigation at 1:25000 scale (Khon, 1997). Research on general geology and Holocene sediments in the coastal Thanh Hoa area is still limited. The research results at the LKTH2 borehole have reflected the sedimentation process in the high terrain area of the Thanh Hoa plain in the Late Pleistocene period (Ha et al., 2019). This result does not fully reflect the Holocene deposition process of the Thanh Hoa Plain. Studies in the Red River Delta have identified two branches of the Late Quaternary incised valley with the most encountered at 60-70 m depth (Lam, 2004), and the incised valley in the Mekong Delta with the most incredible depth > 60 m (Ha, 2015). The incised valley reflects the Holocene deposition process in the coastal Thanh Hoa.

The LKTH6 borehole reached 30 m depth at the edge of the Late Quaternary incised valley in the coastal Thanh Hoa area (Fig. 2). This article is the new results that contribute to clarifying the Holocene sediment process in the coastal Thanh Hoa area.

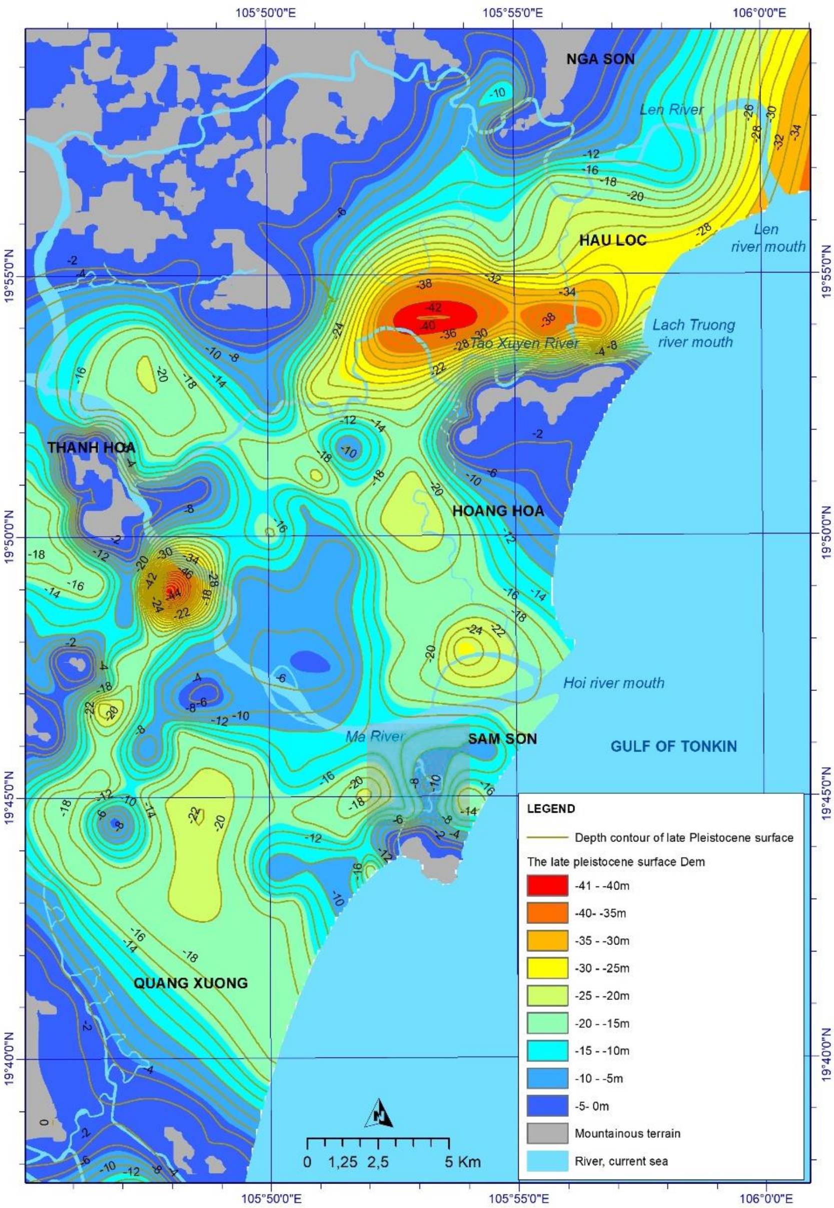

Figure 2. Subaerial exposure surface during the late Pleistocene (Based on 116 core drills in Table 1)

Table 1. The depth of upper late Pleistocene sediment (*Late Pleistocene surface (m) compared to sea level 0)

No	Symbol core	Coordinates		depth (m)	No	Symbol core	Coordinates		depth (m)
		Longitude	Latitude				Longitude	Latitude	
1	KT 33	105.79	198.225	-10.5	59	KT86	105.843	197.436	-16.4
2	KT 49	105.788	197.845	-18.0	60	KT87	105.825	197.214	-17.4
3	KT100	105.894	197.492	-11.5	61	KT91	105.885	197.531	-7.6
4	KT101	105.879	197.443	-15.8	62	KT92	105.875	197.495	-15.2
5	KT103	105.914	197.607	-13.1	63	KT93	105.871	197.406	-7.0
6	KT104	105.907	197.546	-13.6	64	KT94	105.863	197.288	-7.3
7	KT105	105.901	197.432	-15.1	65	KT95	105.859	197.169	-8.5
8	KT12	105.805	198.694	-18.5	66	KT96	105.841	197.168	-16.3
9	KT13	105.797	198.608	-16.4	67	KT97	105.915	197.716	-15.6
10	KT14	105.791	198.545	-15.2	68	KT98	105.908	197.649	-9.0
11	KT15	105.849	198.516	-21.0	69	LH10SS	105.898	19.75	-17.4
12	KT16	105.766	198.279	-18.2	70	LK10HR	105.806	197.763	-4.9
13	KT17	105.758	198.228	-17.4	71	LK11	105.829	199.052	0.0
14	KT21	105.837	198.769	-7.0	72	LK11HR	105.795	19.787	-10.0
15	KT22	105.78	198.266	-8.0	73	LK12	105.791	196.234	-16.0
16	KT23	105.811	198.506	-3.0	74	LK12SS	105.841	197.583	-11.8
17	KT24	105.802	19.857	-15.1	75	LK13	105.897	197.975	-25.5
18	KT25	105.799	198.468	-3.0	76	LK13HR	105.778	197.862	-4.6
19	KT26	105.791	198.357	-4.2	77	LK13SS	105.792	197.648	-6.0
20	KT29	105.766	198.132	-14.6	78	LK14	105.946	198.962	-41
21	KT32	105.79	198.263	-2.4	79	LK14HR	105.757	197.868	-8.0
22	KT34	105.786	19.815	-6.9	80	LK15	106.004	199.837	-26.5
23	KT35	105.769	197.994	-11.6	81	LK15HR	105.772	198.013	-7.4
24	KT40	105.845	198.446	-9.9	82	LK15SS	105.834	197.264	-8.0
25	KT41	105.834	198.344	-16.2	83	LK16	105.912	199.224	-17.4
26	KT43	105.816	198.149	-16.2	84	LK16HR	105.789	198.089	-10.0
27	KT44	105.798	198.157	-6.5	85	LK17HR	105.788	198.038	-11.0
28	KT47	105.782	198.001	-12.1	86	LK17SS	105.781	19.743	-4.0
29	KT48	105.779	197.916	-17.0	87	LK1SS	105.867	197.491	-20.7
30	KT50	105.777	197.793	-26.6	88	LK25HR	105.756	198.367	-19.0
31	KT51	105.776	197.646	-21.0	89	LK27HR	105.762	198.549	-7.0
32	KT53	105.761	197.493	-19.2	90	LK28	105.794	198.949	-19.0
33	KT54	105.86	198.611	-7.6	91	LK2HR	105.795	198.281	-18.2
34	KT55	105.885	198.707	-17.8	92	LK2SS	105.896	197.419	-13.9
35	KT56	105.901	19.872	-13.0	93	LK39	105.965	199.712	-11.7
36	KT57	105.884	198.527	-20.2	94	LK3HR	105.777	198.183	-17.3
37	KT58	105.867	198.354	-18.2	95	LK40	105.973	199.912	-9.2
38	KT59	105.86	198.285	-6.8	96	LK45	105.973	199.489	-12.2
39	KT6	105.772	198.681	-16.5	97	LK4SS	105.845	197.194	-12.8
40	KT60	105.85	198.183	-7.2	98	LK5SS	105.854	197.128	-10.4
41	KT61	105.838	198.056	-6.5	99	LK6HR	105.804	198.034	-10.3
42	KT63	105.816	197.838	-3.4	100	LK6SS	105.849	197.428	-16.4
43	KT64	105.804	197.705	-17.5	101	LK7	105.915	199.731	-12.7
44	KT65	105.793	197.501	-18.5	102	LK7HR	105.789	197.934	-17.6
45	KT66	105.777	197.536	-19.0	103	LK7SS	105.859	19.737	-16.0
46	KT67	105.768	19.728	-19.8	104	LK8SS	105.867	197.266	-19.1
47	KT68	105.761	197.192	-10.0	105	LK9HR	105.818	197.859	-6.4
48	KT7	105.761	198.577	-12.0	106	LKND14-1QT	105.833	196.617	-17.0
49	KT71	105.897	198.389	-18.0	107	LKPT	105.929	199.461	-18.0

No	Symbol core	Coordinates		depth (m)	No	Symbol core	Coordinates		depth
50	KT73	105.873	198.089	-16.4	108	LKTH1	105.893	197.607	-10.0
51	KT74	105.857	197.904	-5.5	109	LKTH2	105.843	197.657	-11.7
52	KT76	105.827	19.76	-17.8	110	LKTH3	105.823	198.195	-10.3
53	KT77	105.810	197.399	-21.9	111	LKTH4	105.758	198.718	-10.1
54	KT79	105.786	197.178	-18.5	112	LKTH5	105.895	198.081	-18.0
55	KT82	105.912	198.165	-14.9	113	LKTH6	105.93	199.144	-26.3
56	KT83	105.887	197.981	-17.0	114	LKTH7	105.884	198.777	-20.8
57	KT84	105.876	197.868	-16.8	115	LKTH8	105.848	198.802	-22.9
58	KT85	105.860	197.602	-14.3	116	LKTH9	105.877	199.026	-41.0

Source: Quan and Chu, 1980; Khon, 1997, Ha and Quang 2022

2. Geological setting

2.1. Meteorological and Hydrological Regime

- River system: Ma River has a total area of 28490 km^2 and is located in the territory of Laos and Vietnam (Hung, 2015; Tai and Cuong, 2017; Trung and Lam, 2014). In Vietnam, the Ma River is located within the administrative boundaries of 5 provinces: Lai Chau, Son La, Hoa Binh, Thanh Hoa, and Nghe An. The length of the mainstream of the Ma River is 522 km. The Ma River has 39 major tributaries and 2 distributaries (Tai and Cuong, 2017). The annual flow in the Ma River is 23-25 billion m^3 (but unevenly distributed). During the three mouths of the flood season, the total flow volume accounts for 17-18 billion m^3 (Chung and On, 2018; Tai and Cuong, 2017).

- Hydrological:

Tides: The coastal area of Thanh Hoa belongs to the irregular diurnal tide regime with a tidal cycle of more than 24 hours a day. In a tidal period, there is also a day when a semi-diurnal tide appears. The high tide time is short from 7 to 8 hours, high tide time (8-9 hours), and the tide time recedes (15-16 hours) daily. At Hoang Tan station (Ma River estuary), the highest tide level is 2.9 m, and the lowest low tide is -1.81m depth. At Lach Sung (Len River mouth) the highest tide level is 2.58 m, and the lowest is -0.97 m depth (Hung, 2015).

Waves: based on wave data at Bach Long Vy (about 190 km from the coast of Thanh Hoa to the N.E.) show that the wave field changes with two seasons: Winter (from December to March): the prevailing wave direction offshore is N.E. with stable frequency from 51 to 70%, wave height reaches 0.5-1.3 m and highest reaches 1.5-6.0 m. In coastal areas, wave direction is N.E. (11%), East (34%), and S.E. (22%), wave height is 0.4-0.9 m, and the highest is 0.75-3.0 m. In winter, the coastal area is most affected by wave directions caused by the N.E. monsoon system. Summer (from June to September): The prevailing wave direction offshore is the South with a stable frequency (37-60%). The wave height reaches 0.8-1.3 m, and the highest reaches 4.0-9.0 m. The prevailing coastal areas are Southeast (24%) and South (20%). These wave directions have a substantial impact on the coastal area. Wave height in summer is much higher than in winter due to the frequent influence of storms and tropical depressions into thunderstorms and whirlwinds (Hung, 2015).

2.2. Geomorphological features

12 participating geomorphological units depict the coastal Thanh Hoa area, and the desolate mountainous terrain (Fig. 1) (Quang et al., 2021; Quang, 2022). The river-formed morpho-sedimentary units are: (1) point bar characterized by grain size finning upward in sediment; (2) Channel bar mainly composed of gray sand silt; (3) Levee formed on two sides of the channel with the composition of yellow gray sand, silty sand; (4) Flood plain with silty clay or clayed silt distributed in a

narrow area along the rivers. The wave-formed morpho-sedimentary units are: (5) Dunes extending in narrow trip quasi-parallel to the coast; (6) Interdune swamps lower than surroundings, consisting of Clay, slit, and sand in small thickness; (7) Sand beach with good sorted and very high content of sand, distributed continuously in the South of the study area; (8) Lagoon plain in form of narrow trip, made up of dark gray silty Clay with organic humus (9) Strand plain covering widely in the study area. The tide-formed morpho-sedimentary units, mainly distributed in the northern part of the study area, include (10) Supratidal flat consisting of Clay and silt; (11) Intertidal flat with alternation of finer (Clay, silty Clay) and coarser (sand, silty sand) grained deposition in 1-2 mm thick beds; (12) Subtidal flat with the main component of sand and silty sand (Quang et al. events, 2021; Quang, 2022).

2.3. Holocene stratigraphy

Holocene sediments in the coastal Thanh Hoa area are divided into two formations:

(1) Thieu Hoa Formation ($Q_2^{1\text{-}2}$ *th*) consists of river-sea (am), sea (m), and sea-marsh (bm) sediments. The Thieu Hoa Formation sediments are distributed in Thanh Hoa, Dong Son, Quang Xuong, and the west of Hoang Hoa, with a 2-4 m topographic elevation. In the East, this sediment is the Holocene. The average thickness of the sediments of the Thieu Hoa Formation ranges from 15-20 m. The Lach Truong estuary area's most significant thickness is up to 41 m (Khon, 1997; Quan and Chu, 1980).

(2) The Thai Binh Formation is divided into two sub-formations: the lower sub-formation ($Q_2^3 th_1$) consisting of sediments of river-sea (am), marine, marsh beach (mb) origin, and the upper stratum (mb). ($Q_2^3 th_2$) includes marsh beach (mb) sediments, sea marsh, and marine origin. The sediments of the Thai Binh Formation are widely distributed in the coastal areas of Hoang Hoa, Sam Son, Quang Xuong and along the major rivers of the Ma river system (Khon, 1997; Quan and Chu, 1980).

2.4. Neo-Tectonic and Dynamic

The Ma River fault system is the main driving force behind the formation of the Thanh Hoa delta in the late Cenozoic. Modern faults include NW-SE faults, NE-SW faults, sub-meridian faults and sub-latitudes. Two critical fault systems in the NW-SE and NE-SW have divided the study area into blocks with different movement mechanisms during the neo-construction period, creating uplift and lowering architectures typical for this region: block Lach Truong mountain uplift, Dong Son block uplift area, Quang Xuong block uplift area, block protruding on Truong Le mountain tectonic downhill foundation, the transition zone between uplift movement and Ma river estuary block (Khon, 1997); Quan and Chu, 1980).

3. Data and methods

The LKTH6 core was carried out at Hoa Loc commune, Hau Loc district, Thanh Hoa province, in 2019. its location of 105°55'43" N and 19°54'55" E. Total of 32 m length of the sediment core was obtained with a sample recovery rate of 78%. In the lab, the core was described in detail by the structural features, color characteristics, plant fragments, biological debris, and the change in grain composition. Forty-seven Grain size samples were analyzed by Sieve and Pipette method; the Spore-pollen analysis (14 samples); Foraminifera (14 samples) were analyzed on Euromex stereo microscope at x10, x20, and 40x magnifications at the Institute of Geology, Vietnam Academy of Science and Technology; Fourteen Diatom samples analyzed on Carl Zeiss biological microscope with magnification x400 and x1000 at the Laboratory of Geology, University of Science, Vietnam National University, Hanoi; clay minerals (3 samples) by X-ray diffraction (XRD), using a Panalytical diffractometer at the Institute of Geology, Vietnam Academy of Science and Technology and ^{14}C isotope age (4 samples) at DirectAMS laboratory, USA.

Grain size analysis method: using a sieve and pipette to determine the percentage content of particles to build a particle accumulation chart and a particle distribution chart to calculate the parameters Medium grain size (Md), degree of sorting (So), Skewness (Sk). Using particle analysis results to classify and determine the sediment's name according to Folk's classification (1954). The variation in grain composition in the cross-section helps to determine the law of sediment distribution in space and time as a basis for explaining the sediment deposition environment.

Methods of paleontological analysis (Spore-pollen, Foraminifera, Diatom):

Spore pollen can be transported by wind or water and deposited with sediments. In sediments, pollen spores are well preserved due to their thin shells, which are resistant to chemical agents. For Cenozoic sediments in general and Quaternary sediments in particular, Spore-pollen is one of the essential paleontological groups in studying stratigraphic establishment and the sedimentary environment containing them.

- Foraminifera are a group of foraminifera. In addition to the significance of stratigraphy, this group of fossils' degree of sorting has great significance in studying the environment of sediment formation.

- Diatom lives in many different environments, floating in marine and freshwater environments and on the bottom in sedimentary basins. Studying the Diatom fossil assemblage is significant in restoring the ancient environment, including the ancient coastal environment (A, Korhola, 2007) because of the richness of species, the ability to preserve good, simple quantitative combinations (Palmer and Abbott, 1986), especially they are sensitive to changes in water environmental factors such as salinity, nitrogen and phosphorus content in water. (R.W, 1986).

Clay mineral analysis method: X-ray diffraction (XRD) determined the clay mineral composition using a Panalytical diffractometer at the Institute of Geology, Vietnam Academy of Science and Technology. The composition and content of clay minerals are indicators of the sediment formation environment.

Radiocarbon dates: ^{14}C age were measured on shells and plant fragments by AMS method at DirectAMS laboratory, USA. Analytical results were calibrated on Calib radiocarbon Calibration Program software, version Valib Rev 8.1.0, Copyright 1986-2020 M Stuiver and PJ Reimer.

4. Results

Based on the sedimentary characteristics and ^{14}C ages, the strata of LKTH6 core were divided into two units. Unit 1 (32-30 m), late Pleistocene sediments consist of highly oxidized reddish-brown, tan-colored laminate silty clay. Unit 2 (30-0 m), Holocene sediments underly unconformity on Unit 1, which divided into ten sedimentary facies as follows (Fig. 3).

4.1. Flood plain silty clay facies

These facies are distributed at 30.0-28.3 m depth, overlain unconformity the latest Pleistocene sediments, and consist of dark gray, greenish gray silt clay, containing few completely decomposed humus-like plants (Fig. 4a1, a2). Clay (58.19-66.67%), silt (33.72-40.45%), Medium grain size (Md): 0.002-0.003 mm, degree of sorting (So): 1.94-2.54, Skewness (Sk)): 1.44-1.90. Sediment containing spores-pollen aggregates characteristic of the freshwater environment, including Polypodiaceae gen. indet., *Polypodium* sp., *Plagiogyria* sp., Poaceae gen. indet., *Myrica* sp., *Carya* sp., Myrtaceae gen. indet. (Fig. 5a, a'). In sediments completely absent of cotyledonous fossils, the absence of cotyledonous fossils indicates that the sediments were deposited in an environment without marine elements or because the sedimentary environment has a significant driving force that is not favorable for fossilization with holes deposited together. The clay mineral composition includes kaolinite 39.1%, illite 38.8%, chlorite 21.0%, and smectite 1.2% (Table 2, Fig. 6c). The high kaolinite content indicates the deposition conditions in the continental environment. At the LKTH6 core, the floodplain clay silt deposits directly covered the patchy, weathered surface of the Late Pleistocene of Vinh Phuc Formation.

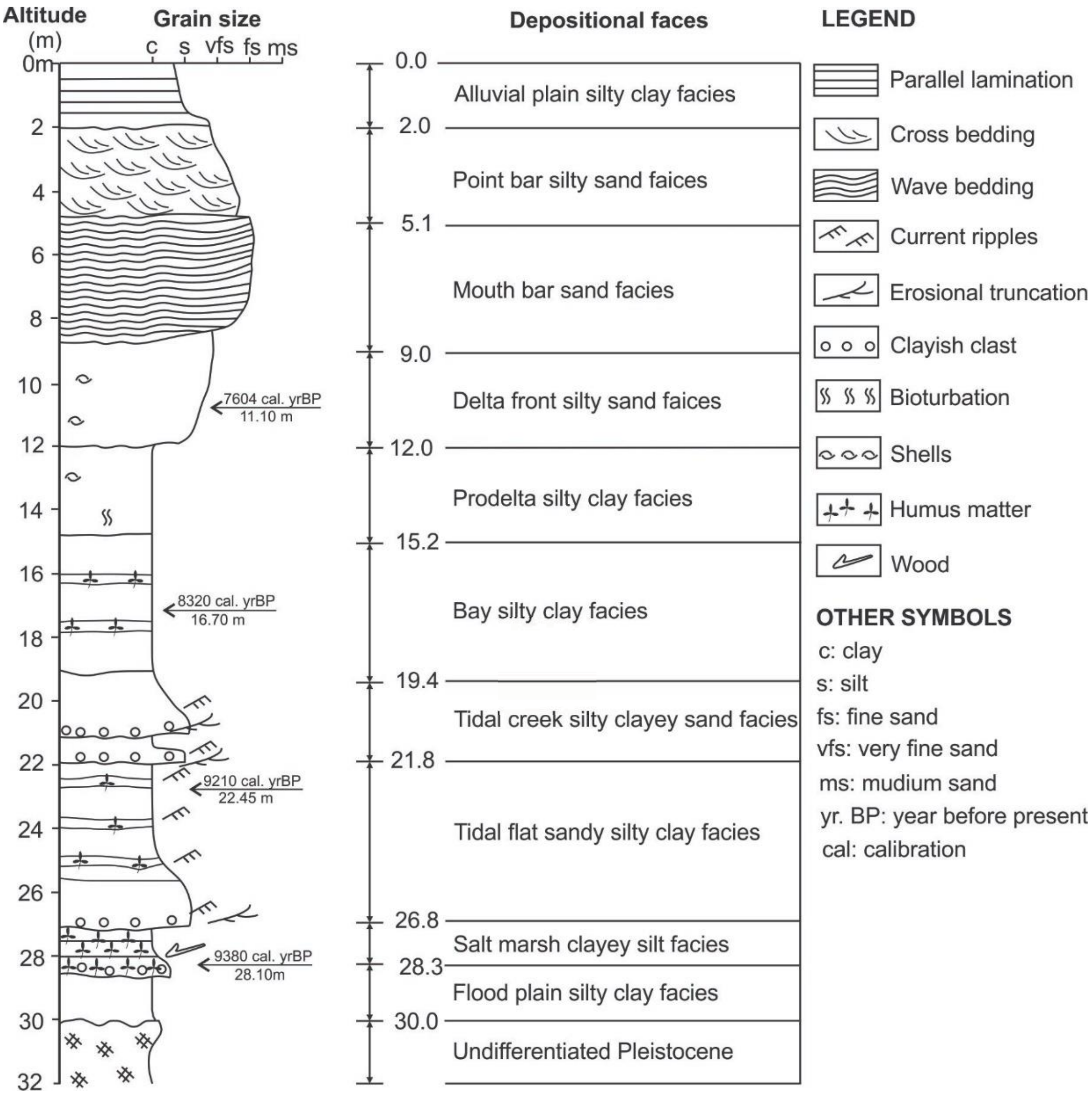

Figure 3. Sedimentary facies of the LKTH6 core

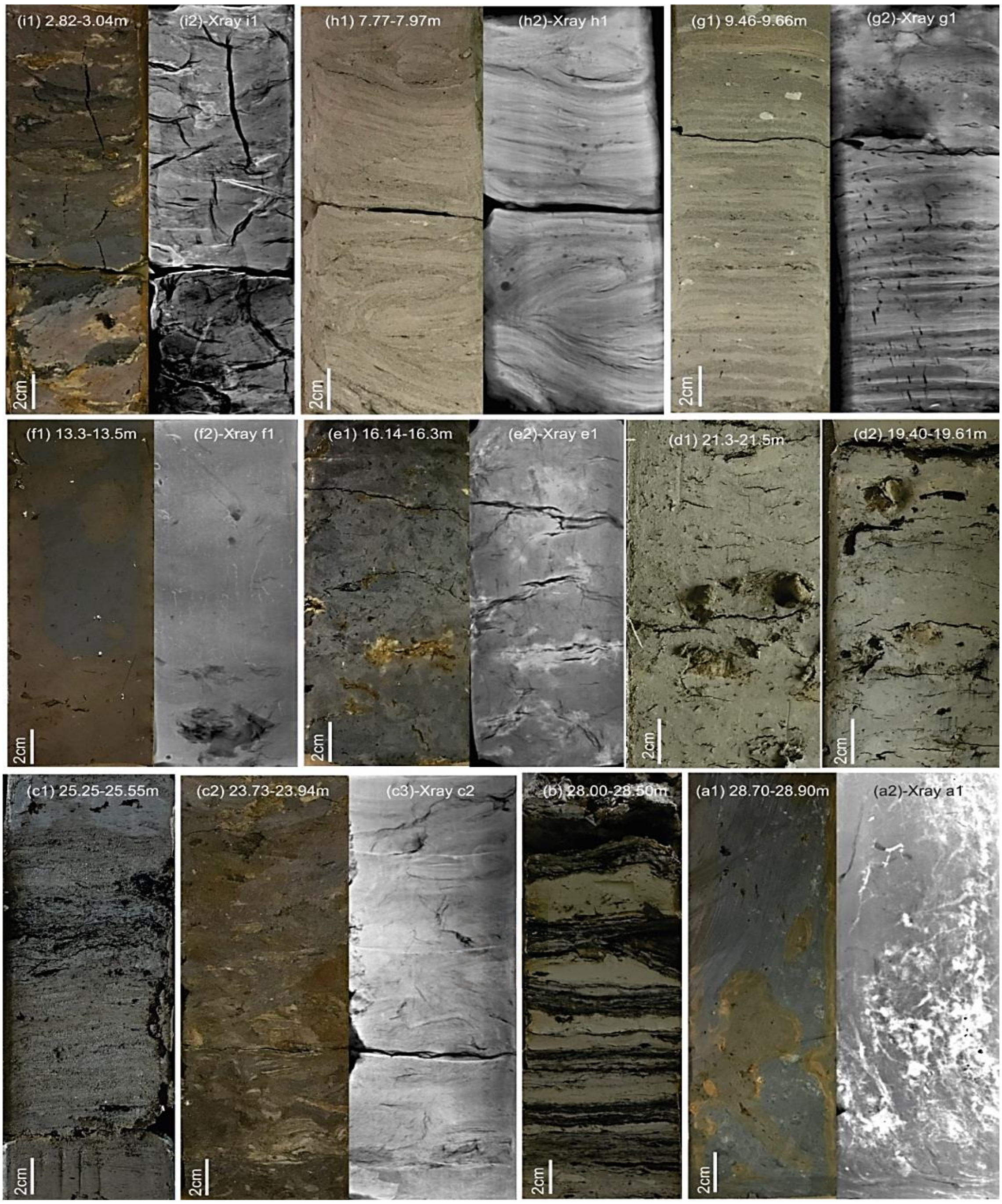

Figure 4. Photographs and radiographs (negatives) of LKTH6 core: Flood plain silty clay (a1-core sample, a2-Xray a1); salt marsh clayey (b); tidal flat sandy silt clay (c1, c2-core sample, c3-Xray c2); creek and branch sandy clay (d1, d2); bay silty clay (e1-core sample, e2- Xray e1); prodelta silty clay (fi-core sample, f2-Xray f1); delta front silty sand (g1-core sample, g2-Xray g1); mouth bar sand (h1-core sample, h2-Xray h1); point bar sandy silt (i1-core sample, i2-Xray i1)

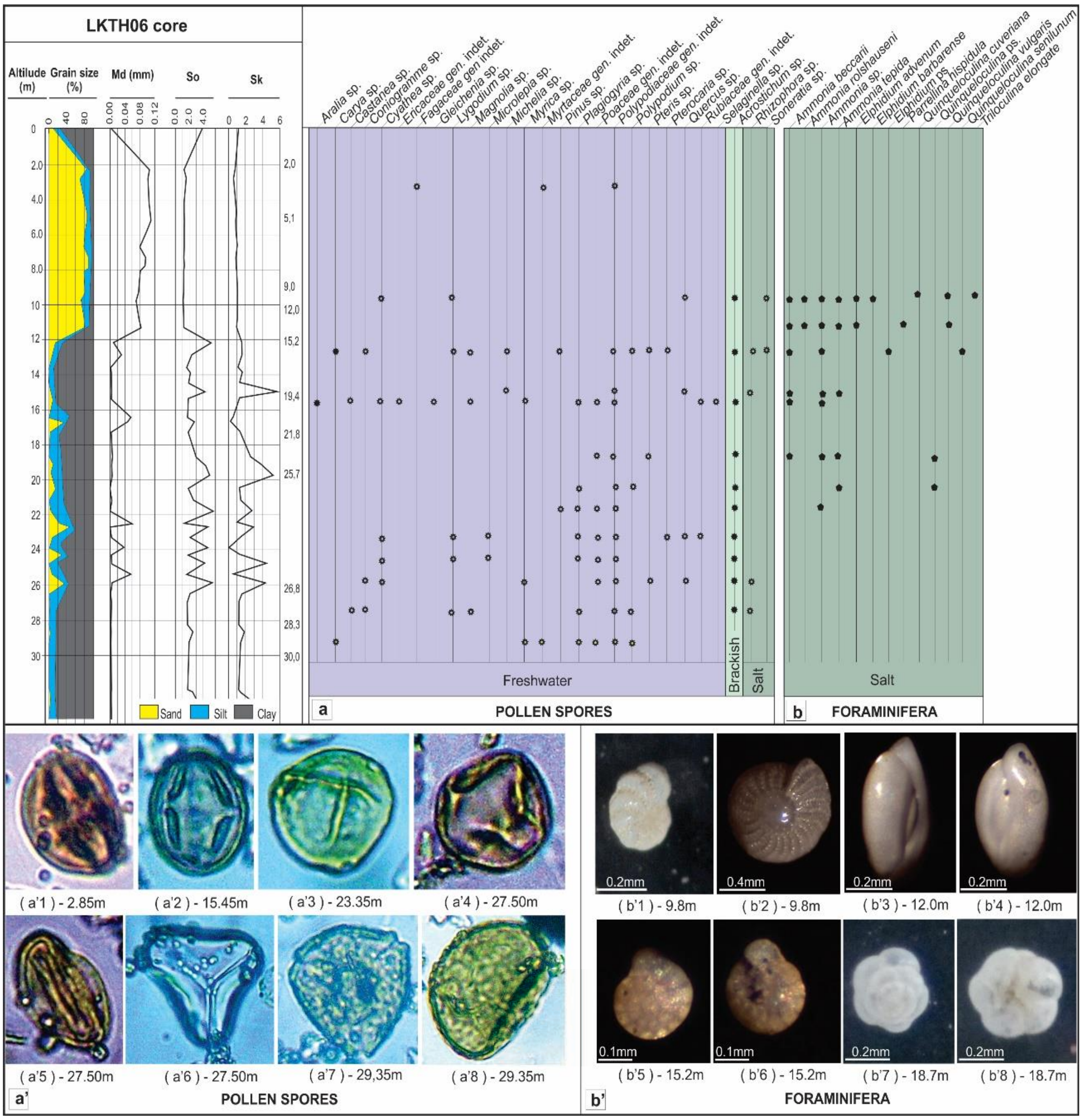

Figure 5. Pollen-spore (a) and foraminifera (b) of the LKTH6 core; Photographs of spores-pollen: (a'1)- Fagaceae *(Facus) (x450)*, (a'2)- Rubiaceae *(Rubia) (x450)*, (a'3)- *Pterocarya* sp. *(x450)*, (a'4)- *Rhizophora* sp. *(x450)*, (a'5)- *Quercus* sp. *(x450)*, (a'6)- *Acrostichum* sp. *(x450)*, (a'7)- *Myrica* sp. *(x450)*, (a'8)- *Polypodium* sp. *(x450);* Photographs of foraminifera: (b'1)- *Elphidium advenum*, (b'2)- *Elphidium barbarense*, (b'3)- *Quinqueloculina semilunum*, (b'4)- *Quinqueloculina semilunum*, (b'5)- *Ammonia beccarii* (backside), (b'6)- *Ammonia beccarii* (belly face), (b'7)- *Ammonia tepida* (back), (b'8)- *Ammonia tepida.*

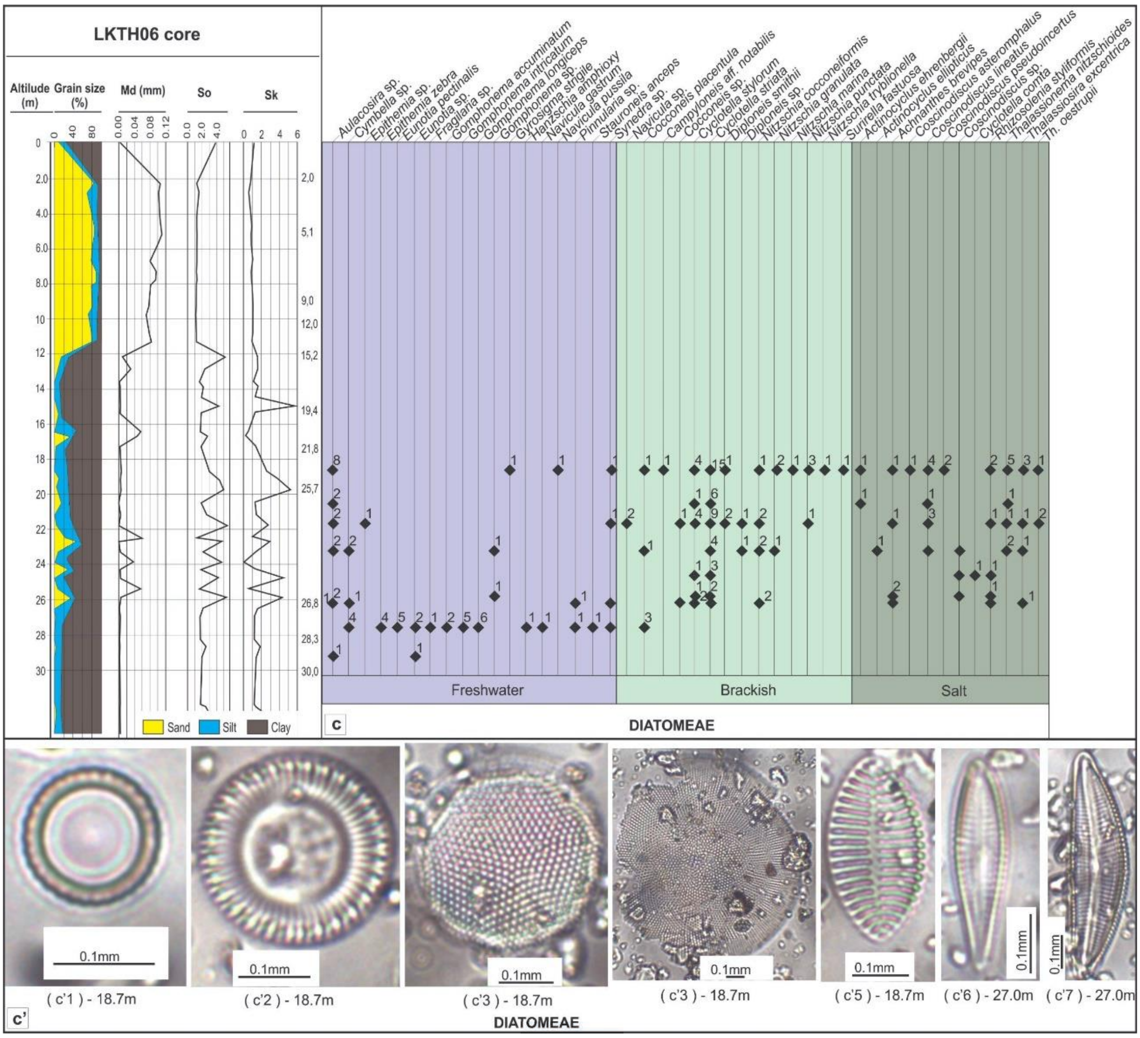

Figure 5 (continued). Diatom (c) of the LKTH6 core; Photographs of Diatomeae: (c'1)- *Aulacosira* sp., (c'2)- *Cyclotella striata* (Kutzing) Grunow, (c'3)- *Thalassiosira excentrica* (Ehrenberg) Cleve, (c'4)- *Coscinodiscus asteromphalus* Ehrenberg, (c'5)- *Nitzschia cocconeiformis* Grunow, (c'6)- *Gomphonema intricatum* Kutzing, (c'7)- *Cymbella* sp.

Table 2. Composition and content of clay minerals oriented by X-ray diffraction method

Symbol	Depth (m)	Mineral composition and content (%)			
		Smectite	Illite	Kaolinite	Chlorite
LKTH6/KVS01	16.75	6.4	**51.0**	30.2	12.5
LKTH6/KVS02	24.85	1.5	**63.3**	21.1	14.1
LKTH6/KVS03	28.85	1.2	38.8	**39.1**	21.0

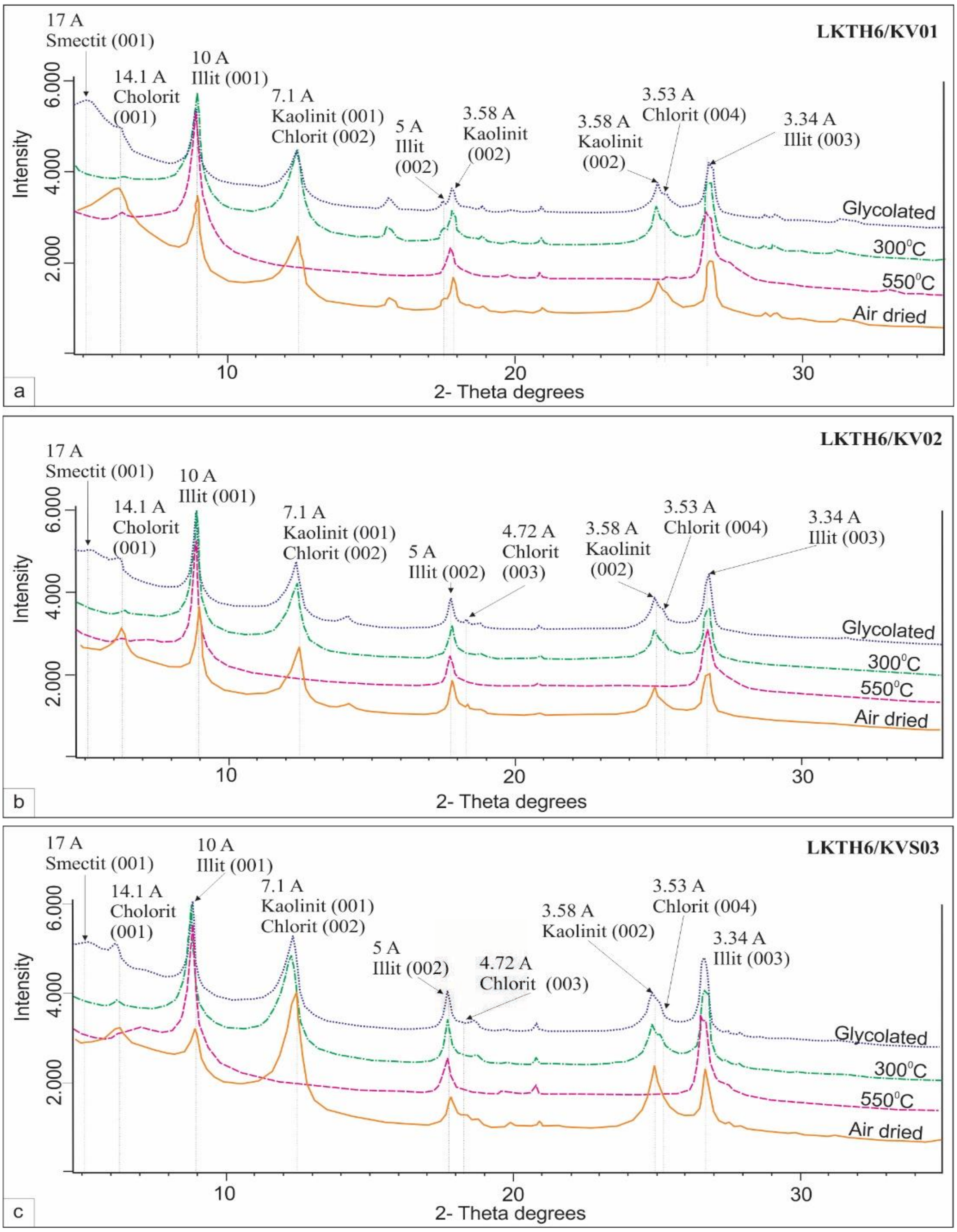

Figure 6. X-ray diffraction pattern of clayey samples of LKTH6 core

4.2. Salt marsh clayey silt facies

Coastal estuaries are affected by river flows and tidal currents, creating favorable conditions for plants to grow along the banks of the estuaries.

This facies is distributed at 28.3-26.8 m depth and characterized by layers of plant humus, thick stems (1-2 cm black, regularly interspersed with layers of gray silt clay) (Fig 4b). Grain-sized content of intercalated silty clay layers: Clay (64.38-65.40%), silt (32.48-35.69%), sand (0-3.0%), Medium grain size (Md): 0.002-0.003 mm; degree of sorting (So): 1.72- 2.05; Skewness (Sk): 1.22-1.62. They contain spores-pollen aggregates in freshwater- brackish-salt environment, where *Acrostichum* sp. lives in a brackish water environment, especially the mangrove species *Rhizophora* sp. (Fig. 5a, a'). In addition, Cocconeis placenta is a benthic species in brackish water in the Diatom assemblage, confirming that the silty clay deposit formations are evenly sandwiched. These plant humus layers are regularly formed in the saline-brackish environment. Results of ^{14}C isotopic age analysis of plant humus (wood) at a 28.10 m depth give an age of 9380 cal. yr BP (Table 3). The sea level has risen to the LKTH6 core position.

Table 3. List of AMS ^{14}C dates

No	Symbol	Symbol in Lab	Depth (m)	Material	Radiocarbon age (yr. BP)	Calibrated age (cal. yr BP)	Mean Calibrated age (cal. yr BP)	Possibility (%)
1	LKTH6/C01	D-AMS 041129	11.00	shell	7320 ± 60	7474-7733	7604	100%
2	LKTH6/C02	D-AMS 041131	16.70	Organic	7545 ± 78	8181-8465	8320	93%
3	LKTH6/C03	D-AMS 041132	22.45	Organic	8198 ± 84	8992-9427	9210	100%
4	LKTH6/C04	D-AMS 041133	28.10	Organic	8365 ± 60	9266-9493	9380	87%
5	LKTH2/C03	D-AMS 024732	7.06	Organic	6951 ±38	7717-7798	7758	77%
6	LKTH2/C04	D-AMS 024733	8.98	Organic	7109 ±39	7928-7971	7950	69%
7	LKTH2/C06	D-AMS 024735	12.37	Organic	7883 ±43	8597-8725	8661	87%

Note: Samples (1-4): This study; Samples (5-7): Previous study (Ha, 2019)

4.3. Tidal flat sandy silty clay facies

These facies appeared at 26.8-21.8 m depth, consisting of gray and dark gray sandy silt abundant plant humus. The silty clay sediments are interspersed with sandy silt and plant humus (Fig. 4c1, c2). In addition, due to the location of LKTH6 in the coastal estuary area, the sediment is often strongly disturbed by the flow (Fig. 4c3). The grain size composed of Clay (31.25-65.61%), silt (34.63-45.70%), and sand (0-29.8%), Medium grain size (Md): 0.003-0.037 mm, degree of sorting (So): 1.85-4.67, Skewness (Sk): 0.15-4.38. Sediment containing spores-pollen aggregates of fresh-brackish-salt water plants, including Polypodiaceae gen. indet., *Acrostichum* sp., *Plagiogyria* sp., *Pinus* sp., Poaceae gen. indet., *Cyathea* sp., *Lygodium* sp., *Microlepia* sp., *Pterocaria* sp., *Quercus* sp., *Rhizophora* sp. (Fig. 5a, a'). Submerged vegetation accounts for 25-30% of the complex, allowing confirmation of sediment origin. Tidal flats of coastal rivers. The occurrence of a diatom assemblage including *Actinocyclus ellipticus*, *Achnanthes brevipes*, *Aulacosira* sp., *Cocconeis placentula*, *Cocconeis* sp., *Coscinodiscus lineatus*, *Coscinodiscus* sp., *Cyclotella comta*, *Cyclotella stylorum*, *Cyclotella striata*, *Diploneis smithii*, *Diploneis* sp., *Epithemia* sp., *Gomphonema* sp., *Navicula* sp., *Nitzschia cocconeiformis*, *Nitzschia punctata, Nitzschia granulata*, *Rhizosolenia styliformis, Synedra* sp., *Thalassionema nitzschioides*, *Thalassiosira excentrica, Thalassiosira oestrupii* indicates a coastal environment (Fig. 5c, c'). Clay mineral composition includes kaolinite 21.1%, illite 63.3%, chlorite 14.1%, and smectite 1.5% (Table 2, Fig. 6b). Illite accounts for over 50% of the hydromica group, always present in the coastal transition zone, bay sea, and shallow sea. The ^{14}C isotope age analysis of plant humus at a depth of 22.45 m gives an age of 9210 cal. yr BP (Table 3).

4.4. Tidal creek and tidal branch silty clayey sand facies

On the tidal flats, tidal creeks and tributaries are often formed. Tidal creeks and tidal branches often excavate and erode the sedimentary formations they pass, leaving coarse-grained bottom sediments to interfere with shell fragments and mudclasts. At the LKTH6 core, the tidal creek and tidal branch, distributed at (21.8-19.4 m) depth, consist of intercalated silty Clay and sand. In the core sample, there are two sets of clasts, the size of the pebbles is 1×1 cm, and the sediments gradually increase in succession (Fig. 4d2). Clay content (5.27-65.15%), silt (35.41-48.33%), sand (0-46.4%), medium grain size (Md): 0.003-0.061 mm, degree of sorting (So): 1.26-5.38, Skewness (Sk): 0.98-5.23. The sediments contain spore-pollen fossils characteristic of a brackish-salt environment, including *Acrostichum* sp., *Rhizophora* sp. (Fig. 5a, a'). The foraminifera were indicated a tidal habitat by a wide salinity species, including *Ammonia* sp., *Ammonia tepida, Nonion* sp., *Quinqueloculina* sp.. Diatom assemblage appears marine and brackish species, representing the coastal environment including *Actinocyclus divisus, Aulacosira* sp., *Coscinodiscus lineatus*, *Cyclotella striata, Cyclotella stylorum, Thalassionema nitzschioides* (Fig. 5c, c').

4.5. Bay silty clay facies

The sea level rise causes the estuary area to become a bay. The aquatic environment is quite deep and quiet, depositing fine-grained sedimentary formations. These facies distributed at depth (19.4-15.2 m) consist of greenish-gray, yellowish-gray silty Clay and organic layers commonly interlaminated with silty Clay. (Fig. 4 e1, e2). Grain size of sediment is characterized by Clay (37.00-66.97%), silt (33.11-45.44%), sand (0-9.60%), Medium grain size (Md): 0.003-0.047 mm, So: 1.84-2.92, and Skewness (Sk): 0.27-2.54. The sediment contains spore-pollen aggregates, including Polypodiaceae gen. indet., *Pteris* sp., *Selaginella* sp., *Cyathea* sp., *Plagiogyria* sp., *Acrostichum* sp., *Gleichenia* sp., Ericaceae gen. indet., *Myrica* sp., *Magnolia* sp., Rubiaceae gen. indet. , Poaceae gen. indet., *Aralia* sp., *Castanea* sp (Fig. 5a, a'). These are broad-salt species, adapted to large changes of salt in water, including *Ammonia* sp., *Ammonia beccarii.*, *Quinqueloculina* sp., *Ammonia tepida*. Diatom assemblage includes *Actinocyclus ehrenbergii, Achnanthes brevipes, Aulacosira* sp., *Campyloneis* aff. *notabilis*, *Cocconeis placentula, Coscinodiscus asteromphalus, Coscinodiscus lineatus, Coscinodiscus pseudoincertus, Cyclotella stylorum, Cyclotella striata, Diploneis smithii, Gyrosigma strigile, Navicula pussila, Nitzschia cocconeiformis, Nitzschia granulata, Nitzschia marina, Nitzschia punctata, Nitzschia tryblionella, Rhizosolenia styliformis, Surirella fastuosa, Synedra* sp., *Thalassionema nitzschioides, Thalassiosira excentrica, Thalassiosira oestrupii* (Fig. 5c, c'). Clay minerals include kaolinite 30.2%, illite 51.0%, 12.5% chlorite, and 6.4% smectite (Table 2, Fig. 6a). More than 50% illite of the hydromica group is always present in coastal transition zones, gulf seas, and shallow seas. The result of the ^{14}C isotope age is 8320 cal. yr BP of plant humus at 16.7 m depth (Table 3).

4.6. Prodelta silty clay facies

This facies is distributed at a depth (15.2-12.0 m), consisting of dark gray Clay, gray-brown silty Clay, and silty sand interspersed (Fig. 4f1, f2). The grain size of sediment is characterized by Clay (40.26-73.46%), silt (26.91-44.54%), sand (0-14%), Medium grain size (Md): 0.002-0.03 mm; degree of sorting (So): 1.63-2.36, Skewness (Sk): 1.13-5.98. reservoirs containing spore-pollen aggregates of coastal estuarine mangroves including *Cyathea* sp., *Lygodium* sp., Polypodiaceae gen. indet., *Polypodium* sp., *Pteris* sp., *Coniogramme* sp., *Lygodium* sp., *Acrostichum* sp., *Magnolia* sp., *Pterocarya* sp., *Michelia* sp., *Rhizophora* sp., *Sonneratia* sp., *Pinus* sp., *Quercus* sp., (Fig. 5a, a'). Fossils of the Foraminifera are mainly wide salinity species, including *Ammonia beccarii*, *Ammonia tepida*, *Ammonia* sp., *Quinqueloculina semilunum*, *Elphidium* sp..

4.7. Delta front silty sand facies

This facies distributed at depth (12.0-9.0 m) is composed of fine-grained sand, dark gray, and light gray silt interspersed with parallel lamination silty clay (Fig. 4g1, 1g2 . Grain size is characterized by silt (18.0-26.7%), and (73.3-81.9%), Medium grain size (Md): 0.071-1.04 mm, degree of sorting (So): 1.15-1.22, Skewness (Sk): 0.96-1.04. A low number of foraminifera species was recorded with some species adapted to the wide salinity of shallow sea near the shore, including, including *Ammonia* sp., *Ammonia beccarii*., *Ammonia rolshauseni*., *Ammonia tepida*., *Parrellina hispidula*., *Elphidium advenum*., *Quinqueloculina vulgaris*. Pollen and spore include *Lygodium* sp., *Cyathea* sp., *Acrostichum* sp., *Soneratia* sp., *Quercus* sp. (Fig. 5b, b'). The radiocarbon dating ^{14}C of 7604 cal. yr BP of shells at 11.0m depth (Table 3).

4.8. Mouth bar Sand facies

Wave dynamics dominate the estuaries. The material from the continent is screened and regenerated by waves and tides. The fine materials are carried away while the coarser particles are deposited at the mouth of the river, creating a barrier. The sand dune facies at the LKTH6 borehole have relatively fine sediments, dark gray to yellowish gray. Sediment-containing shells appear in the lower part and no longer appear, with a parallel wavy layered structure, silt (11.8-24.0%), sand (75.9-88.1%), Medium grain size (Md): 0.082-0.81 mm, degree of sorting (So): 1.22-1.26, Skewness (Sk): 0.9-0.98. The sand dunes have a thickness of 3.9 m, a distribution of depth (9.0-5.1 m) (Fig. 4h1, 1h2).

4.9. Point bar silty sand faices

Rivers with a high degree of curvature often form a meandering belt, with the river bed freely winding to the sides within the confines of this belt, forming point bars (Emery and Keith Myers, 1996). The sediments along the bed are gray, dark gray silty sand, with a lot of plant humus distributed sporadically, not in aggregates, and sometimes gray-brown silty Clay (Figs. 4i1, 1i2). The coastal sediments have an oblique layered structure. The composition is silt (157-31.9%), sand (68.1-84.3%), Medium grain size (Md): 0.102-0.11 mm; degree of sorting (So): 1.24-1.28, Skewness (Sk): 0.58-0.88. The sediment of silty sand along the bed is 3.1 m thick, distributed in depth (5.1-2.0 m). Sediment containing spores-pollen aggregates characteristic of freshwater environment including Polypodiaceae gen. indet., Myrtaceae gen. indet., Fagaceae gen indet. (Fig. 5a, a').

4.10. Alluvial plain silty clay facies

The delta developed to the sea, and rivers completely dominated the upper part of the delta. At the LKTH6 borehole, the alluvial plain sediments are distributed from a depth of 2.0m to the present surface of the delta. The sediments are mainly silty clay formations with Clay (56.2%), silt (34.2%), and sand (9.6%), Medium grain size (Md): 0.003 mm; degree of sorting (So): 3.87, Skewness (Sk): 1.15. The sediment contains the freshwater diatom assemblage including *Aulacosira* sp., *Eunotia clevei, E. pectinalis, Eunotia monodon*.... Freshwater spore-pollen collection includes *Polypodium* sp., *Quercus* sp., Polypodiaceae gen. indet., *Pinus* sp., *Taxodium* sp., *Pteris* sp., *Lygodium* sp., (Fig. 5c, c').

5. Discussions

The process of sea level change during the Holocene:

The sediment facies of the LKTH6 core is typical as strata of incised valley fill, with a good record of sea level change during postglacial.

The time of the beginning of the Flandrian transgression is about 18000 yr. BP and the rapid rise is about 15000-14000 yr. BP corresponds to the Late Pleistocene period (Nghi and Toan, 2000; Tanabe et al., 2003a, 2003b). The time of the beginning of the Flandrian transgression is about 18000 yr. BP and the rapid rise is about 15000-14000 yr. BP corresponds to the Late Pleistocene period (Nghi and Toan, 2000; Tanabe et al., 2003a, 2003b). The duration of sea level fluctuations during the Holocene was divided into three stages by previous studies on Red River Delta: stage I (9000-6000 yr. BP), stage II (6000-4000 yr. BP), and stage III (4000-0 yr. BP) (Hanebuth et al., 2000; Tanabe et al., 2003a, 2003b) during the Holocene transgressive, still-stands and regressive, respectively. The sea level rise on the Red River Delta at about 10000-8000 yr. BP (Hori et al., 2004; Huang et al., 1987; Lam and Boyd, 2000; Mathers and Zalasiewicz, 1999; Tanabe et al., 2003a) peaked at 6000-5000 yr. BP with a maximum elevation of (+5)-(+6 m) above present sea level (Lam and Boyd, 2001).

In the coastal Thanh Hoa area, the Flandrian sea level rise reached to the incised valley of this study area, resulting in the salt marsh sediment facies formed at 28.3-26.8 m depth of LKTH6 core, radiocarbon date of 9380 cal. yr BP, corrilatively the beginning of stage I of the Flandrian sea level rise in the Red River Delta (Fig. 7). Around 9200 yr. BP, the intertidal sediments were from 26.8 m to 21.8 m depth and formed estuary-bays sediments at 8.300 yr. BP, the LKTH6 site was submerged in the sea, forming bay silty clay sediments. At around 8600 yr. BP, the sea level rose overlying the subaerial exposure, It was recorded by the occurrence of the intertidal sediments at the LKTH2 core of 12.7-10.4 m depth, radiocarbon dated ^{14}C of 8661 cal. yr BP. The sediment supply from the continental to the seaward exceeded the sea level rise rate at around 7600 yr. BP leading to the delta accumulated including prodelta, delta front, and delta plain sediment facies were identified at the LKTH6 core.

Maximum transgression at 6000 yr. BP, after this time, 5000 yr. BP is a regression (Lam and Boyd, 2001; Tanabe et al., 2003a, 2003b, 2006; Tamura et al., 2012; Nghi et al., 2002). The search area has strong wave dynamics, forming coastal estuarine dunes. The delta seaward, the LKTH6 core, is not influenced by the sea. At this time, the erosion activities of the river develop, forming the riverbed and floodplain sediments.

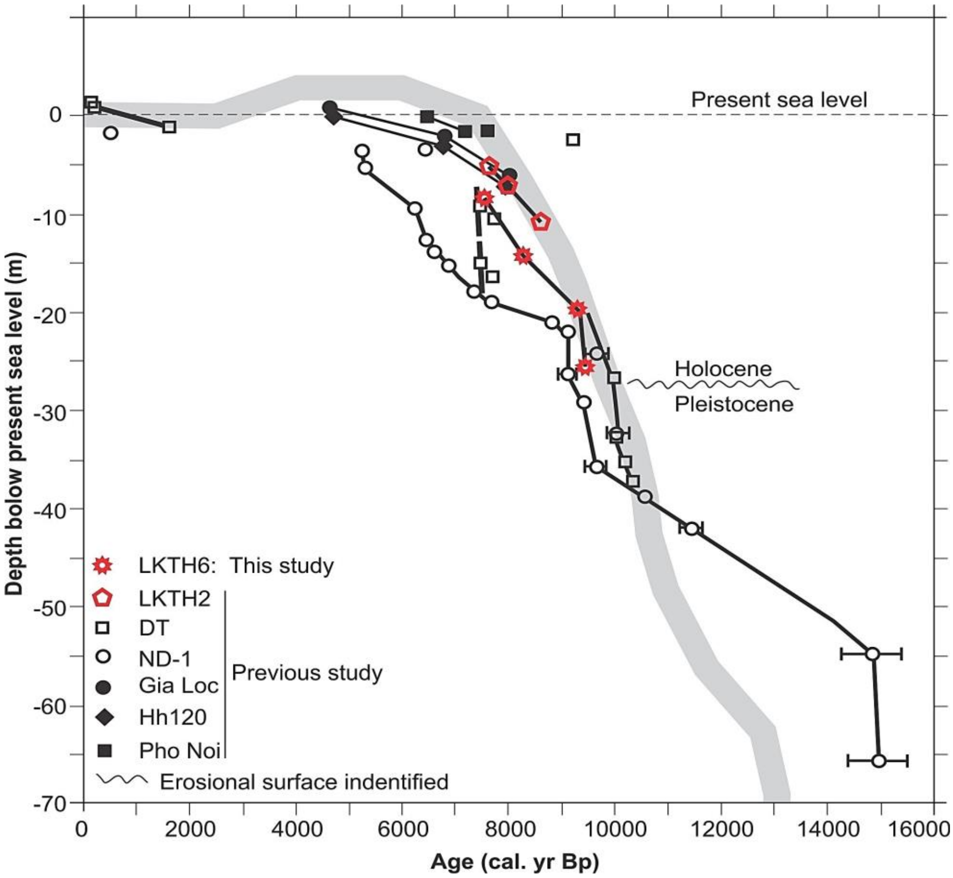

Figure 7. Accumulation curves of Ma River Delta and Red River Delta of Vietnam. Age uncertainties correspond to 1 sigma estimate. Sea-level curve for Eastern Vietnam sea during the past 20 kyr (Tanabe et al., 2006); DT (Tanabe et al., 2003a), ND-1 (Tanabe et al., 2003b), HH120 (Lam and Boyd, 2000), Gia Loc and Pho Noi (Nghi and Toan, 2000) in (Tanabe et al., 2000)., 2003a), and LKTH2 (Ha et al., 2019)

The rate of the Flandrian sea level rise

According to research results in the Red River Delta, it is confirmed that the average sea level fluctuation rate in stage I increases from -15 m to +3 m above the current sea level at a rate of 6 mm/year. In stage II, the sea level is relatively stable. During stage III, the sea level gradually decreased from +3 m above the current sea level at an average rate of 0.6±0.1 mm/year (Hanebeth et al., 2000). In the Holocene, sea level rise was relatively fast, reaching 10-12 mm/year (Ky, 1980; Lam, 2003; Nghi, 2000), between 10,000 and 8000 yr. BP the sea flooded the Red River Delta (Hori et al., 2004; Huang et al., 1987; Lam and Boyd, 2000; Mathers and Zalasiewicz, 1999; Tanabe et al., 2003a) with a rate of 9-12 mm/year (Huang et al., 1987) at 7000 yr. BP, the rate of sea level rise is only about 2-4 mm/year (Lam, 2004; Lam and Boyd, 2001) after 6000 yr. BP, the sea recedes slowly sinusoidally (Lam and Boyd, 2001).

In the coastal Thanh Hoa area, the results of ^{14}C age in the sediments marked the shoreline of the Flandrian sea level rise, including the salt marsh, tidal flat facies at the LKTH6 core, and intertidal flats sediments at the LKTH2 core (Fig. 8). Sediment was deposited from 28.1 m to 22.5 m depth over 170 years, corresponding to a sedimentation rate of

33.2 mm/year. At 550 years, from 22.5 m to 11.1 m depth, the corresponding sedimentation rate is 12.2 mm/year. The sampling locations of the ^{14}C age analysis are the location of sea level. As a result, the sedimentation rate corresponds to the sea level rise rate.

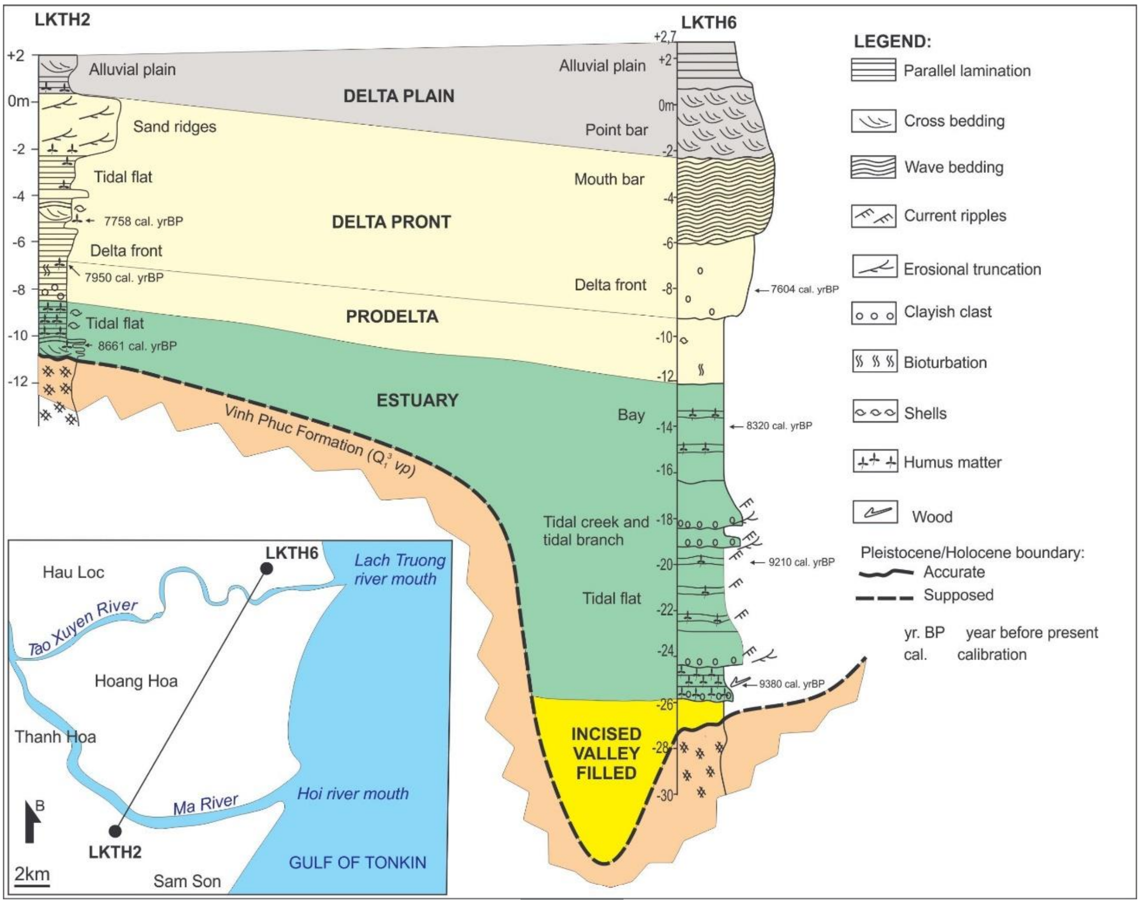

Figure 8. Diagram of the connection between LKTH6 and LKTH2 cores sedimentary environment in the coastal Thanh Hoa area

Depositional environment

The depositional environment in the Late Quaternary incised valley of the Red River Delta changed from the bottom being river and river-sea formations to the uppermost being salt marsh sediments, bays formations, deltaic sedimentary formations, and alluvial sediments (Lam, 2004). In the study area, the results of paleontological classification (spores-pollen, foraminifera, diatom) shed light on the Holocene sediment deposition environment in the coastal Thanh Hoa area. Freshwater and brackish diatom species are mixed together, demonstrating a nearshore sedimentary environment with characteristics from continental to swampy (Fig. 5c). As freshwater diatom species declined, it shows that there was seawater intrusion into the continent during that time. Fossil species of foraminifera occur abundantly in saltwater environments. A few can be found in brackish water or bay but not in freshwater environments (Fig. 5b). For spores-pollen, sedimentary formations deposited in freshwater environments are all characterized by the absence of mangrove and brackish plants. The delta environment is often formed in the estuary and coastal conditions, so the marine-influenced environment is characterized by pollen spore complexes with different proportions of mangrove plant pollens (Fig. 5a).

6. Conclusions

The Holocene depositional environment in the coastal Thanh Hoa area is reflected in 10 sedimentary facies with four groups of formation environment: (1) The incised valley-filled facies, characterized by freshwater environment as the floodplain silt facies. (2) The estuarine facies typical for the transitional and marine environments, including and the salt marsh clayey silt facies, the tidal creek and tidal branch silty sand facies; the tidal flats clayey silt sand facies; the bays silty clay facies. (3) The deltaic facies typical for the delta environment includes the prodelta silty clay facies, the delta front sandy silt facies, and mouth bar sand facies. (4) The alluvial facies typical for the freshwater environment include the point bar silty sand facies and the alluvial plain silty clay facies.

The transgression after the last glacial resulted in the incised valley filled up by fluvial sediments before 9380 yr. BP and drowned completely the valley around 9380-8000 yr. BP. The process accumulation of delta occurred since 7600 yr. BP.

The Holocene accumulation rate in the LKTH6 core of period 9400-9200 yr. BP, 9200-8300 yr. BP, 8300-7600 yr. BP, and 7600 yr. BP to present are 33.2 mm/year, 6.5 mm/year, 7.8 mm/year, and 1.5 mm/year, respectively.

Acknowledgments

We thank the Vietnam Academy of Science and Technology (VAST) for supporting the code KHCBĐ.02/20-22 project financially. The article is a result of the project code KHCBĐ.02/20-22, "Research on the sedimentary facies and Holocene evolution of the Ma river delta."

References

A. Korhola, 2007. Diatom methods, Data Interpretation. Encyclopedia of Quaternary Science. Scott A. Elias. (Ed), 1, 494-507.

Chung L.N., On T.V., 2018. Application of one-dimensional hydraulic model to evaluate the trend of low flow variation in Ma river basin. Irrigation and Environmental Science and Technology, 60, 41-47.

Emery D., Keith Myers, 1996. Sequence Stratigraphy. BP Exploration, Stockley Park Uxbridge, London, 264p.

Ha V.V., 2015. Characteristics of sedimentary environment and history of Holocene geological development in the coastal estuary of the Mekong River system (PhD. thesis). Academy of Science and Technology, Hanoi, 142p.

Ha V.V., Lam D.D., Duong N.T., Cuc N.T.T., Quang N.M., Tha H.V., Min N.T., Tuan D.M., Tung D.X., Chi G.T.K., 2019. Holocene sedimentary facies in coastal plain of the Song Ma Delta, Thanh Hoa Province. Vietnam J. Earth Sci., 41(3), 229-239. https://doi.org/10.15625/0866-7187/41/3/13832.

Hanebuth T., Stattegger K., Grootes P.M., 2000. Rapid flooding of the Sunda Shelf: a late-glacial sea-level record. Science, 288, 1033-1035.

Hori K., Tanabe S., Saito Y., Haruyama S., Nguyen V., Kitamura A., 2004. Delta initiation and Holocene sea-level change: example from the Song Hong (Red River) delta, Vietnam. Sedimentary Geology, 164, 237-249.

Huang Z., Li P., Zhang Z., Zong Y., Qin Y., Zhao S., 1987. Sea-level changes along the coastal area of South China since Late Pleistocene. Late Quaternary Sea-level Change. China Ocean Press, Beijing, 142, 154.

Hung N.T., 2015. Research and assess the impact of the upstream lake on changes in the downstream and coastal estuaries of the Ma river system and propose solutions to limit adverse impacts for sustainable development (Project title). Account KC08-32/11-15). National Key Laboratory of River and Sea Dynamics (KLORCE), Vietnam Institute of Irrigation Science, 433p.

Khon H.V., 1997. Report on urban geological investigation of Thanh Hoa city, scale 1:25000. Geospatial Center. Hanoi, 187p.

Period H.N., 1980. Sea advance stages in the Quaternary period and their shelf in the territory of North Vietnam. Collection of reports of the Geosciences Conference celebrating the 25th anniversary of Vietnam's Geology, 128-129.

Lam D.D., 2004. The formation and evolution of the Late Quaternary section of the Red River Delta. Petroleum Magazine, 7, 9-18.

Lam D.D., 2003. Evolutionary history of Holocene sediments in the Red River Delta (PhD thesis). University of Science - Vietnam National University, Hanoi, National Library of Hanoi, 122p.

Lam D.D., Boyd W.E., 2001. Some facts of sea-level fluctuation during the Late Pleistocene-Holocene in Ha Long Bay and Ninh Binh area (in Vietnam). Vietnam J. Earth Sci., 23(2), 86-91.

Lam D.D., Boyd W.E., 2000. Holocene coastal stratigraphy and model for the sedimentary development of the Hai Phong area in the Red River delta, north Viet Nam. Journal of Geology (Series B), 15, 18-28.

Mathers S., Zalasiewicz J., 1999. Holocene sedimentary architecture of the Red River delta, Vietnam. Journal of Coastal Research, 314-325.

Nghi T., 2000. Sedimentary evolution and paleogeography in the Pliocene-Quaternary period Vietnam's territory and territorial sea. Journal of Geology, A, 19-29.

Nghi T., Nhuan M.T., Van Ngoi C., Hoekstra P., Weering V.T., VDen Bergh J.H., Thanh D.X., Nguyen N.D., Van Phai V., 2002. Holocene sedimentary evolution, geodynamic and anthropogenic control of the Balat river mouth formation (Red River-delta, northern Vietnam). Zeitschrift fur Geologische Wissenschaften, 30, 157-172.

Nghi T., Toan N.Q., 2000. Development history of deposits in the Quaternary of Vietnam. The weathering crust and Quaternary sediments in Vietnam. Department of Geology and Minerals of Vietnam, Hanoi, 177-192.

Palmer A.J.M., Abbott W.H., 1986. Diatoms as indicators of sea-level change, in: van de Plassche O. (Ed.), Sea-Level Research: A Manual for the Collection and Evaluation of Data. Springer Netherlands, Dordrecht, 457-487. https://doi.org/10.1007/978-94-009-4215-8-16.

Quan D.T., Owner N.T., 1980. Report on the establishment of geological and mineral maps in Thanh Hoa-Vinh newspaper, scale 1:200000. Geospatial Center. Hanoi, 335p.

Quan N.C., Hung P.V., 2016. Characteristics of dynamic geomorphology of coastal-river mouth zones of Ma river, Thanh Hoa province. Vietnam J. Earth Sci., 38(1), 59-65.

Quang N.M., 2022. Evolutionary history of Holocene sediments in the coastal area of Thanh Hoa (PhD thesis). Academy of Science and Technology, Hanoi National Library, 138p.

Quang N.M., Ha V.V., Tan M.T., Ban T.X., Dien T.N., Tuan D.M., Tung D.X., Min N.T., Tha H.V., Chi G.T.K., 2021. Geomorphological sedimentary characteristics in the coastal area of Ma river delta, Thanh Hoa province. Vietnam Journal of Marine Science and Technology, 21, 283-298. https://doi.org/10.15625/1859-3097/15995.

R.W. B., 1986. Diatom analysis. In: Handbook of Holocene Paleoecology and Palaeohydrology. Edited by Berglund, B.E., J. Wiley &Sons Ltd., New York, 527-570.

Tai N.V., Cuong V.M., 2017. Research anti-flooding solution for the Chu - Ma river system in Thanh Hoa province. Journal of Water Resources & Environmental Engineering, 58, 122-129.

Tamura T., Saito Y., Bateman M.D., Nguyen V.L., Ta T.O., Matsumoto D., 2012. Luminescence dating of beach ridges for characterizing multi-decadal to centennial deltaic shoreline changes during Late Holocene, Mekong River delta. Marine Geology, 326, 140-153.

Tanabe S., Hori K., Saito Y., Haruyama S., Kitamura A., 2003a. Song Hong (Red River) delta evolution related to millennium-scale Holocene sea-level changes. Quaternary Science Reviews, 22, 2345-2361.

Tanabe S., Hori K., Saito Y., Haruyama S., Sato Y., Hiraide S., 2003b. Sedimentary facies and radiocarbon dates of the Nam Dinh-1 core from the Song Hong (Red River) delta, Vietnam. Journal of Asian Earth Sciences, 21, 503-513.

Tanabe S., Saito Y., Vu Q.L., Hanebuth T.J., Ngo Q.L., Kitamura A., 2006. Holocene evolution of the Song Hong (Red River) delta system, northern Vietnam. Sedimentary Geology, 187, 29-61.

Trung N.Q., Lam N.X., 2014. Performance of reservoirs operation to the low-flow in lower Ma river basin. Journal of Water Resources & Environmental Engineering, 44, 88-94.